



**Providing Choice & Value**

Generic CT and MRI Contrast Agents



CONTACT REP

# AJNR

This information is current as of July 17, 2025.

## **Can Shunt Response in Patients with Idiopathic Normal Pressure Hydrocephalus Be Predicted from Preoperative Brain Imaging? A Retrospective Study of the Diagnostic Use of the Normal Pressure Hydrocephalus Radscale in 119 Patients**

J.F. Carlsen, A.D.L. Backlund, C.A. Mardal, S. Taudorf, A.V. Holst, T.N. Munch, A.E. Hansen and S.G. Hasselbalch

*AJNR Am J Neuroradiol* published online 30 December 2021

<http://www.ajnr.org/content/early/2021/12/30/ajnr.A7378>

# Can Shunt Response in Patients with Idiopathic Normal Pressure Hydrocephalus Be Predicted from Preoperative Brain Imaging? A Retrospective Study of the Diagnostic Use of the Normal Pressure Hydrocephalus Radscale in 119 Patients

J.F. Carlsen, A.D.L. Backlund, C.A. Mardal, S. Taudorf, A.V. Holst, T.N. Munch, A.E. Hansen, and S.G. Hasselbalch

## ABSTRACT

**BACKGROUND AND PURPOSE:** The Normal Pressure Hydrocephalus Radscale is a combined scoring of 7 different structural imaging markers on preoperative brain CT or MR imaging in patients with idiopathic normal pressure hydrocephalus: callosal angle, Evans Index, Sylvian fissure dilation, apical sulcal narrowing, mean temporal horn diameter, periventricular WM lesions, and focal sulcal dilation. The purpose of this retrospective study was to assess the performance of the Normal Pressure Hydrocephalus Radscale in distinguishing idiopathic normal pressure hydrocephalus shunt responders from nonresponders.

**MATERIALS AND METHODS:** The preoperative MR imaging and CT scans of 119 patients with idiopathic normal pressure hydrocephalus were scored using the Normal Pressure Hydrocephalus Radscale. A summary shunt-response score assessed within 6 months from ventriculoperitoneal shunt surgery, combining the effect on cognition, gait, and urinary incontinence, was used as a reference. The difference between the mean Normal Pressure Hydrocephalus Radscale for responders and nonresponders was tested using the Student *t* test. The area under the curve was calculated for the Normal Pressure Hydrocephalus Radscale to assess shunt response. To ascertain reproducibility, we assessed the interobserver agreement between the 2 independent observers as intraclass correlation coefficients for the Normal Pressure Hydrocephalus Radscale for 74 MR imaging scans and 19 CT scans.

**RESULTS:** Ninety-four (79%) of 119 patients were shunt responders. The mean Normal Pressure Hydrocephalus Radscale score for shunt responders was 8.35 (SD, 1.53), and for nonresponders, 7.48 (SD, 1.53) ( $P = .02$ ). The area under the curve for the Normal Pressure Hydrocephalus Radscale was 0.66 (range, 0.54–0.78). The intraclass correlation coefficient for the Normal Pressure Hydrocephalus Radscale was 0.86 for MR imaging and 0.82 for CT.

**CONCLUSIONS:** The Normal Pressure Hydrocephalus Radscale showed moderate discrimination for shunt response but cannot, on its own, be used for selecting patients with idiopathic normal pressure hydrocephalus for shunt surgery.

**ABBREVIATIONS:** AUC = area under the curve; CA = callosal angle; DESH = disproportionately enlarged subarachnoid space hydrocephalus; EI = Evans index; iNPH = idiopathic normal pressure hydrocephalus; MMSE = Mini-Mental State Examination; NPH = normal pressure hydrocephalus; PVWML = periventricular WM lesions

The pathophysiology of idiopathic normal pressure hydrocephalus (iNPH) remains largely enigmatic.<sup>1,2</sup> Equally enigmatic are the mechanisms of the only known effective treatment, shunting of the CSF.<sup>3</sup> In light of these shortcomings in our understanding, the

diagnosis of iNPH, as suggested by international guidelines, is based on the combined evaluation of iNPH symptoms, brain imaging, and CSF pressure dynamics.<sup>4</sup> Nevertheless, even after a thorough clinical work-up, a substantial number of patients with iNPH do not benefit from shunt surgery.<sup>5,6</sup> Although generally considered a minor and safe neurosurgical procedure, complications following shunt surgery are not uncommon, including postoperative hematoma, shunt infection, and subdural hematomas arising from over-drainage.<sup>6,7</sup> Weighing the chance of shunt response against the risk of complications is a prime challenge for attending neurologists and neurosurgeons.

Preoperative brain imaging has long been used to establish dilation of the brain ventricles in patients with iNPH.<sup>8,9</sup> In addition, preoperative imaging is used to rule out other types of degenerative

Received June 13, 2021; accepted after revision October 7.

From the Department of Radiology (J.F.C., C.A.M., A.E.H.), Department of Neurology (S.T., S.G.H.), Danish Dementia Research Centre, and Department of Neurosurgery (A.V.H., T.N.M.), Rigshospitalet, Copenhagen University Hospital, Copenhagen, Denmark; Department of Radiology (A.D.L.B.), Hospital of North Zealand, Hillerød, Denmark; Department of Clinical Medicine (T.N.M., A.E.H.), University of Copenhagen, Copenhagen, Denmark; and Department of Epidemiology Research (T.N.M.), Statens Serum Institut, Copenhagen, Denmark.

Please address correspondence to Jonathan Frederik Carlsen, MD, Department of Radiology, Rigshospitalet, Copenhagen University Hospital, Blegdamsvej 9, 2100 Copenhagen OE, Denmark; e-mail: Jonathan.frederik.carlsen@regionh.dk  
<http://dx.doi.org/10.3174/ajnr.A7378>

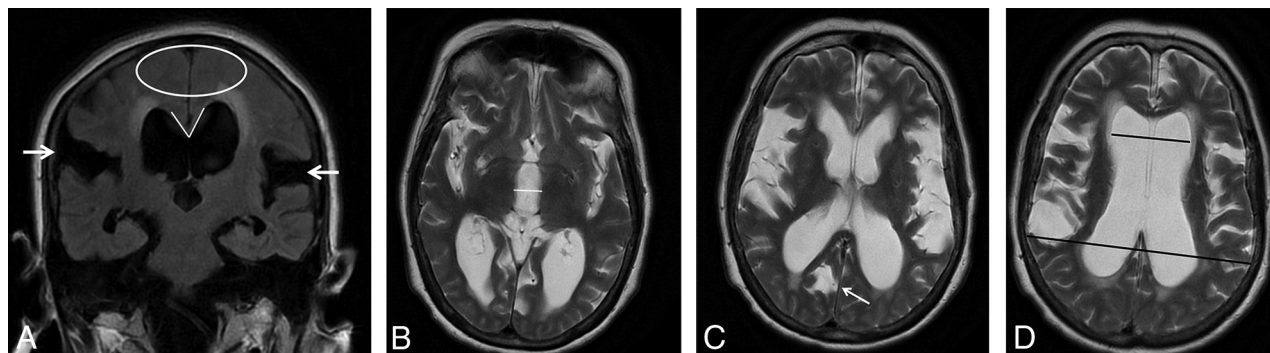


**FIG 1.** MR imaging of a 79-year-old female shunt-responder with an NPH Radscale score of 11. A, Coronal FLAIR image shows marked bilateral Sylvian fissure dilation (white arrows), apical narrowing of sulci (white ellipse), a narrow CA (65°), and marked periventricular hyperintensities. B–D, Axial T2 images at different levels show measurement of third ventricle diameter (white line), sulcal dilation (white arrow), and measurements used for the Evans ratio calculation (black lines).

brain disease, vascular disease, and other types of hydrocephalus before shunt surgery.<sup>9</sup> Several studies have tried to use anatomic imaging markers for predicting shunt response, with varying results.<sup>10–12</sup> These imaging markers include measurements of the callosal angle (CA), Evans index (EI), and temporal horn diameter and evaluation of the presence of disproportionately enlarged subarachnoid space hydrocephalus (DESH), focal sulcal dilation, and focal ventricle bulging. Recently, the Normal Pressure Hydrocephalus (NPH) Radscale, a composite score based on evaluations of 7 different anatomic imaging markers, has been proposed as a predictor of shunt response.<sup>13</sup> The NPH Radscale has been shown to have a good correlation with the severity of iNPH symptoms in a randomly selected group of 168 volunteers older than 65 years of age.<sup>14</sup> Furthermore, the NPH Radscale had a high area under the curve (AUC) for discerning healthy, age-matched adults from iNPH shunt responders.<sup>13</sup> No studies using the NPH Radscale to discern iNPH shunt responders from nonresponders have been published.

In this retrospective study, we aimed to evaluate the usefulness of the NPH Radscale performed on preoperative brain imaging to predict shunt response assessed 6 months after the operation.

## MATERIALS AND METHODS

### Inclusion of Patients and Preoperative Evaluation

The patients included in this retrospective study underwent shunt surgery for NPH at the Department of Neurosurgery, Copenhagen University Hospital, from 2013 to 2020. Approval of retrospective recording of patient data was given by the hospital direction board. All data were recorded from the electronic patient journal and the hospital radiology information system/PACS.

In the study inclusion period, 133 patients were consecutively diagnosed with probable or possible NPH according to clinical guidelines and, consequently, received a ventriculoperitoneal shunt.<sup>15</sup> All patients were evaluated at an interdisciplinary conference between clinicians from the Memory Clinic at the Danish Dementia Research Center and the Department of Neurosurgery, Rigshospitalet, Copenhagen University Hospital, before referral to surgery. The evaluation was based on the presence of iNPH symptoms, including gait disturbance, radiologic characteristics, and results of CSF dynamic measurements obtained whenever possible. These included a lumbar infusion test with measurement of

resistance to outflow and, in some, supplemented by a lumbar tap test with removal of 40 mL of CSF with prior and postobjective evaluation of gait (CELDA System; Likvor). The infusion test and the lumbar tap test were regarded as supportive, not imperative, for decisions about shunting, especially in patients with possible iNPH.<sup>16</sup> Major urogenital, musculoskeletal, or neurologic comorbidities were recorded before the operation.

### Excluded Patients

Brain imaging had been performed in different hospitals with differing protocols. Eleven patients without either an available brain CT or MR imaging performed within 1 year before surgery were excluded. The remaining 122 brain scans were assessed for eligibility, and 3 MR imaging scans with no T2 or FLAIR sequences were deemed insufficient and were excluded. Finally, 119 patients, 20 with CT scans and 99 with MR imaging scans were included. Of these 119 patients, 114 patients had undergone a preoperative lumbar infusion test and 55 had undergone a lumbar tap test as part of the clinical work-up.

### Brain Image Assessment

All scans were assessed by 1 neuroradiologist with 10 years' experience (J.F.C.). To ascertain reproducibility, 2 independent readers (A.D.L.B. and C.A.M., respectively), also assessed 74 random MR imaging scans and 19 CT scans. The 2 additional readers were radiology residents in their last year of residency. All readings were performed blinded to the other readers' evaluations and shunt-response evaluations.

The 7 imaging parameters that compose the NPH Radscale were assessed in accordance with Kockum et al<sup>14</sup> (Fig 1). For CA measurements, a coronal plane perpendicular to the intercommissural plane was reconstructed for both MR imaging and CT when not available.<sup>17</sup> Periventricular white matter lesions (PVWML) were assessed on T2 and/or FLAIR images for MR imaging. All other assessments were performed on available sequences and reconstructions.

The CA and the mean temporal horn diameter were measured in degrees and millimeters, respectively. The presence of focally enlarged sulci was noted as either present or not. Narrowing of the apical sulci was assessed as 0 = normal or wider than normal, 1 = slight compression/parafalcine compression,

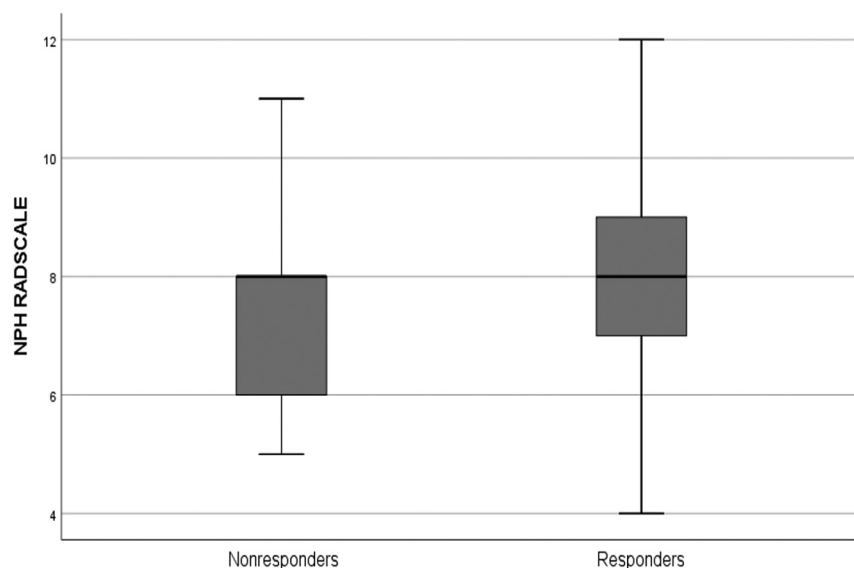


**FIG 2.** A boxplot of NPH Radscale values (y-axis) for responders and nonresponders, respectively. The thick black line is the median; and box upper and lower margins are 75th and 25th percentiles, respectively. Whiskers represent upper and lower ranges.

and 2 = definite compression. Sylvian fissure dilation was rated as present or not. PVWML were evaluated as either 0 = normal, including capping and pencil-thin lining, 1 = increased PVWML, and 2 = confluent areas of PVWML.

In addition to the imaging parameters used for NPH Radscale scoring, readers measured third ventricle diameter in millimeters and assessed ventricular focal bulging.<sup>18</sup> Furthermore, readers assessed the presence of DESH if apical sulci were disproportionately narrow compared with Sylvian fissure dilation.

### Shunt-Response Evaluation

Shunt-response evaluation was performed at outpatient follow-up visits at the Memory Clinic at the Danish Dementia Research Center approximately 6 months after shunt surgery. Gait and cognition were evaluated by using a 10-m gait test and the Mini-Mental State Examination (MMSE).<sup>19</sup> Urinary continence was evaluated by interviewing patients and/or caregivers. Gait and continence were scored by 8- and 6-point scales, respectively.<sup>20</sup> Changes in gait and continence were evaluated as the following: 1) worsening = increase of the score by 1 or more, 2) no effect = no change in scores, 3) moderate effect = a decrease in score by 1, and 4) substantial effect = a decrease in the score by  $\geq 2$ . Changes in cognition were evaluated as the following: 1) worsening = a decrease in the MMSE score by 2 or more, 2) no effect = change by  $-1$  to  $+1$ , 3) moderate effect = an increase in the score by 2, and 4) substantial effect = an increase in the score by  $\geq 3$ . The evaluations for gait, continence, and MMSE were then each scored on a scale from  $-1$  to 2: worsening =  $-1$ , no change = 0, moderate effect = 1, and substantial effect = 2. A summary shunt response score from  $-3$  to 6 was accordingly obtained.

Shunt response was defined as a summary shunt response score of  $\geq 1$ . Due to the retrospective design of the study, postoperative objective measures for gait and cognition were available in

only approximately 80% of the patients. In the remaining patients, scores were obtained by interviewing patients and/or caregivers.

Complications within 1 year from the operation in the form of shunt revision due to shunt malfunction or displacement, shunt revision due to overdrainage, overdrainage without shunt revision, as well as infection, stroke, or death due to shunt surgery were recorded.

### Statistics

Statistics were performed using SPSS, Version 25.0 (IBM). Means are presented as mean (SD); medians are presented as median (range). The Student *t* test with nonequal variances assumed was used to test distributions among continuous data. Distributions of binary variables were tested using the  $\chi^2$  test. For ranked data, a Wilcoxon rank test was performed. Logistic regression was used to test among patient age, sex,

comorbidities, CA, EI, narrowing of apical sulci, Sylvian fissure dilation, DESH, third ventricle diameter, mean temporal horn diameter, ventricular focal bulging, focally enlarged sulci, and PVWML; shunt response was the outcome. To test the robustness of the logistic regression, we performed the same analyses for the entire patient cohort and then twice more on patients randomly assigned to 2 groups with 60 and 59 patients in each group.

Receiver operating characteristic curves were performed for continuous data, and the AUCs were calculated. For the CA, the AUC was calculated for 180 degrees  $-CA$ , because the CA is inversely proportional to the likelihood of shunt response. The Youden index was calculated for the NPH Radscale to find the optimal cutoff.

To assess interrater variability, we calculated intraclass coefficients,  $\kappa$  values, and Spearman rank coefficients for continuous, binary, and ranked data, respectively, and evaluated them according to Landis and Koch.<sup>21</sup>

### RESULTS

Of the 119 patients included in the study, 78 (65.5%) were men and 41 (34.5%) were women. The median age was 77 years (range, 55–90 years). The mean MMSE score was 25.25 (SD, 4.17). The mean time from preoperative imaging to the operation was 190 (SD, 89) days.

The mean summary shunt response score was 2.06 (SD, 1.68). Of 119 patients, 94 (79.0%) were shunt responders. Comorbidities were registered for 77 (65%) patients. There was no significant difference in the distribution of comorbidities between responders, 61 of 94 (65%), and nonresponders, 16 of 25 (64%) ( $P = .93$ ).

The median NPH Radscale score for the entire cohort was 8 (range, 4–12). The median score for shunt responders was 8 (range, 4–12), and the median score for nonresponders was also 8 (range, 5–11) (Fig 2). Complications were seen in 39 (33%)

**Table 1: Distribution of different imaging parameters for the entire population for responders and nonresponders**

	Score	Total	Responders	Nonresponders	P Value
Patients (No.)		119	94	25	
EI <sup>a</sup>		0.39 (0.046)	0.39 (0.046)	0.38 (0.046)	.28 <sup>c</sup>
CA <sup>a</sup>		73.0 (17.4)	71.9 (16.7)	77.2 (19.7)	.23 <sup>c</sup>
Third ventricle diameter <sup>a</sup>		14.2 (3.14)	14.3 (3.00)	14.1 (3.72)	.75 <sup>c</sup>
Mean temporal horn diameter <sup>a</sup>		8.14 (2.40)	8.38 (2.40)	7.26 (2.22)	.03 <sup>c</sup>
NPH Radscale <sup>a</sup>		8.17 (1.56)	8.35 (1.53)	7.48 (1.53)	.02 <sup>c</sup>
DESH <sup>b</sup>	Present	60 (50.4%)	49 (52.1%)	11 (44%)	.47 <sup>d</sup>
	Not present	59 (49.6%)	45 (47.9%)	14 (56%)	
Focal bulging	Present	14 (11.8%)	12 (12.8%)	2 (8.0%)	.73 <sup>e</sup>
	Not present	105 (88.2%)	82 (87.2%)	23 (92.0%)	
Focally enlarged sulci <sup>b</sup>	Present	22 (18.5%)	17 (18.1%)	5 (20.0%)	.78 <sup>e</sup>
	Not present	97 (81.5%)	77 (81.9%)	20 (80.0%)	
Sylvian fissure dilation <sup>b</sup>	Present	101 (84.9%)	83 (88.3%)	18 (72.0%)	.05 <sup>e</sup>
	Not present	18 (15.1%)	11 (11.7%)	7 (28%)	
Narrow sulci <sup>b</sup>	2	47 (39.5%)	29 (30.9%)	4 (16.0%)	.19 <sup>f</sup>
	1	39 (32.8%)	30 (31.9%)	9 (36.0%)	
	0	33 (27.7%)	35 (37.2%)	12 (48.0%)	
PVWML <sup>b</sup>	2	55 (46.2%)	47 (50.0%)	8 (32.0%)	.16 <sup>f</sup>
	1	47 (39.5%)	34 (36.2%)	13 (52.0%)	
	0	17 (14.3%)	13 (13.8%)	4 (16.0%)	

<sup>a</sup> Continuous data are presented as means (SD).

<sup>b</sup> Categorical and ordinal data are presented as No. (%).

<sup>c</sup> Student *t* test.

<sup>d</sup>  $\chi^2$  test.

<sup>e</sup> Fisher exact test.

<sup>f</sup> Mann-Whitney *U* test.

**Table 2: Interrater correlations for continuous evaluations for MR imaging and CT**

	MR Imaging (n = 74)			CT (n = 19)		
	ICC	LB	UB	ICC	LB	UB
EI	0.914	0.863	0.946	0.974	0.932	0.990
CA	0.934	0.895	0.958	0.856	0.626	0.945
Mean temporal horn diameter	0.943	0.909	0.964	0.917	0.784	0.968
Third ventricle diameter	0.918	0.869	0.948	0.966	0.911	0.987
NPH Radscale	0.858	0.774	0.910	0.819	0.531	0.930

**Note:**—LB indicates lower bound; UB, upper bound; ICC, intraclass correlation coefficient.

patients. More nonresponders, 16 of 25 (64%), than responders, 23 of 94 (24%), experienced complications ( $P < .001$ ).

### Preoperative Imaging Findings and Shunt Response

All patients had an EI of  $\geq 0.3$ . Means and SDs for all imaging parameters are presented in Table 1. The NPH Radscale, mean temporal horn diameter, and Sylvian fissure dilation were significantly different between responders and nonresponders.

In the logistic regression analysis, only Sylvian fissure dilation and mean temporal horn diameter were significantly correlated with shunt response ( $P = .017$  and  $P = .028$ ). All other covariates were not significantly correlated with shunt response. For the logistic regression performed in the 2 groups of evenly and randomly distributed patients, Sylvian fissure dilation and the Evans index were significantly correlated with shunt response in the first group ( $P = .018$  and  $P = .038$ ), while mean temporal horn diameter was the last remaining variable in the second group, though it was not significantly associated with shunt response ( $P = .068$ ).

The AUC was 0.66 for the NPH Radscale, range 0.54–0.78, ( $P = .02$ ), 0.60 for the CA, range 0.47–0.72, ( $P = .06$ ), 0.59 for the EI, range 0.46–0.73, ( $P = .07$ ), 0.64 for mean temporal horn

diameter, range 0.53–0.76, ( $P = .06$ ), and 0.54 for third ventricle diameter, range 0.40–0.67, ( $P = .07$ ). The Youden index for the NPH Radscale was 0.239, yielding a sensitivity and specificity of 0.48 and 0.76, respectively, at a cutoff for shunt response of  $\geq 9$ . The AUC for the NPH Radscale for the 80 patients without complications was 0.59, range 0.36–0.83, ( $P = .35$ ).

### Interobserver Agreement

Interoperator variability was assessed for both MR imaging and CT (Tables 2–4). For all continuous assessments, agreement was either excellent or good for both MR imaging and CT. For all categorical assessments, agreement was good or fair, except for focal bulging, which showed no agreement, and PVWML, which showed excellent agreement for CT scans.

### DISCUSSION

This is the first study to evaluate the ability of the NPH Radscale to discern iNPH shunt responders from nonresponders. Although the average NPH Radscale score for shunt responders was significantly higher than for nonresponders, there was only moderate discrimination between the 2 groups, with an AUC =



**Table 3: Kappa statistics for binary categorical evaluations for MR imaging and CT**

	MR Imaging (n = 74)			CT (n = 19)		
	$\kappa$	UB	LB	$\kappa$	UB	LB
DESH	0.569	0.402	0.736	0.607	0.247	0.967
Focal bulging	0.354	0.090	0.617	−0.145	−0.282	−0.006
Focally enlarged sulci	0.617	0.393	0.841	0.650	0.292	1.008
Sylvian fissure dilation	0.617	0.393	0.841	0.477	0.025	0.979

**Note:**— $\kappa$  Indicates Kappa statistics; LB, lower bound; UB, upper bound; DESH, disproportionately enlarged subarchmoid space hydrocephalus.

**Table 4: Spearman rank statistics for non-binary categorical evaluations for MR imaging and CT**

	MR Imaging (n = 74)			CT (n = 19)		
	Spearman Rank	UB	LB	Spearman Rank	UB	LB
Narrow sulci	0.626	0.464	0.747	0.787	0.518	0.914
PVWML	0.691	0.550	0.794	0.826	0.596	0.930

**Note:**—LB indicates lower bound; UB, upper bound; pvWML, periventricular white matter hyperintensities.

0.66. Interoperator agreement for the NPH Radscale was excellent for MR imaging and good for CT.

The NPH Radscale was proposed by Kockum et al,<sup>14</sup> in 2018. It is a composite score based on quantitative and qualitative structural brain image assessments. Although originally evaluated on brain CT, all the imaging parameters have frequently been assessed separately on brain MR imaging in other studies.<sup>18,22,23</sup> Indeed, interobserver and intraobserver variability has been reported for MR imaging and CT previously by the same group, showing good agreement for both.<sup>24</sup>

The NPH Radscale has shown good discrimination between shunt responders and a healthy population of individuals older than 65 years of age.<sup>13</sup> In this study, brain CT was performed no more than 8 days before the operation, and the median NPH Radscale score for shunt responders was 10, compared with 8 in our study. Because no data on nonresponders are presented, it can only be guessed whether the difference lies in the timing and quality of preoperative imaging and the resulting NPH Radscale assessment, in different quantifications of shunt response, or in a genuine difference among the studied populations. A very recent study of 100 possible or probable patients with iNPH undergoing a lumbar tap test showed that the NPH Radscale could not satisfactorily discriminate between patients responding to the tap test and those who did not.<sup>25</sup> Although the lumbar tap test is only a surrogate measure of actual shunt response, this finding is in line with the data presented here.

There is no consensus or guidelines concerning the definition of shunt response or when it should be assessed. We found a shunt response in 80% of patients, which is in line with findings in most larger studies.<sup>18,26,27</sup>

Our findings suggest that the structural changes traditionally described in patients with iNPH cannot, on their own, account for the reversibility of iNPH symptoms. Both nonresponders with high NPH Radscale scores and responders with low NPH Radscale scores were observed. The moderate AUC was not attributable to a skewed distribution of complications between responders and nonresponders because the AUC for patients without complications was similar to that for the whole group. Previous studies have tried to predict shunt response from preoperative anatomic brain imaging, but the results are heterogeneous.<sup>10–12</sup> One study investigating

a similar, composite anatomic score in 50 patients with iNPH showed a difference between shunt responders and nonresponders on a group level but did not report on diagnostic accuracy.<sup>28</sup> In concordance with our data, this finding may suggest that other pathophysiologic mechanisms not visible on structural brain imaging may underlie the response to shunting observed in some patients with iNPH.<sup>29</sup> Furthermore, the response to shunting is associated with compliance to physical training after the operation, which was not accounted for in this study.<sup>30</sup>

Several studies on advanced MR imaging and iNPH have been published. Some studies have focused on aqueductal flow to predict shunt response. Discouragingly, most studies found no discrimination for shunt response with aqueductal flow, though it was reduced after the operation.<sup>31,32</sup> Perfusion imaging has been applied to predict shunt response, suggesting either no discrimination or lowered medial frontal cortex or cingulate gyrus blood flow.<sup>33–35</sup> The studies were, however, too small to warrant any firm conclusions. The findings for both aqueductal flow and brain perfusion imaging emphasize that although some physiologic parameters may be skewed in patients with iNPH, their reversibility following shunt surgery does not correlate with the clinical shunt response.

Another aspect to consider in patients with iNPH is the timing of both symptom onset and the advent of structural changes and how the reversibility of symptoms relates to these time points.

In a small study of brain imaging in patients with iNPH, both the EI of >0.3 and third ventricle diameter were shown to be enlarged and increasingly enlarged in the years before symptom onset.<sup>36</sup> In another study, some patients with asymptomatic ventriculomegaly developed symptoms of iNPH during a follow-up period of 3 years, while another study found clinical and structural progression after 1 year in patients with asymptomatic ventriculomegaly.<sup>37,38</sup> Nonshunted patients with slight iNPH symptoms have, however, shown little progression in an earlier study.<sup>39</sup> These findings support the notion that even though structural brain changes are correlated with and may precede iNPH symptomatology, they cannot, on their own, predict the reversibility of iNPH symptoms.

Recently artificial intelligence has been used to measure volumes of different anatomic brain regions in shunt responders versus nonshunted patients, with good results.<sup>40</sup> Also, a support-

vector machine–based algorithm has been shown to reliably predict an anatomic NPH pattern on brain imaging as defined by a consensus of 4 neuroradiologists, and a deep learning network has been trained to discern patients with NPH from those with Alzheimer disease and healthy controls in a small study population.<sup>41,42</sup> No studies have examined whether artificial intelligence can be used to separate iNPH shunt responders from nonresponders, but this could be a method to extend the utility of structural brain imaging beyond the interpretative skills of neuroradiologists.

### Strengths and Limitations

This study was performed in a single center with a standard setup and long experience in iNPH evaluation. All radiologic evaluations were performed by the same experienced neuroradiologist. The major limitation is the retrospective design of the study, with missing data on objective measurement of outcomes for a subset of patients. However, these data were obtained by interviews of the next of kin and caregivers, ensuring no loss to follow-up. Furthermore, brain imaging was performed in different hospitals, with varying times from shunt surgery and scan protocols. This feature may have hampered the diagnostic potential of the images. However, predefined inclusion criteria for the sequences included in MR images were used, and we found that a consistent image evaluation was feasible. Therefore, the interrater agreement for most parameters, including the NPH Radscale, was good and comparable with that in earlier studies.<sup>24</sup> For logistic regression analyses, there is a risk of collinearity when assessing multiple imaging parameters to diagnose the same pathophysiology on the same brain scan. To test the robustness of the analyses, we performed them first on the entire cohort and then on all patients randomized to 2 groups. The variables that came out significant for the whole group, came out as significant in the first of the split groups and as the last, insignificant parameter before exclusion in the second split group, indicating that the findings were robust to some extent. Collinearity should, however, still be considered for these kinds of analyses.

It is well-known that MR imaging is better for assessing WM vascular disease, but because PVWML are part of the NPH Radscale evaluation, we chose to classify them uniformly for this analysis.

Also, the limited follow-up time of 6 months does not allow us to associate imaging findings with long-term outcomes. Possibly, better outcome measures, including cognitive tests and gait or balance measures, could have been obtained with prospective evaluation.

### CONCLUSIONS

In this study, the use of the NPH Radscale on preoperative imaging yielded moderate discrimination for shunt response. We conclude that currently, the NPH Radscale cannot, on its own, be used to select patients for shunt surgery. Further prospective evaluations should be performed to ascertain the usefulness of the NPH Radscale.

**Disclosure forms** provided by the authors are available with the full text and PDF of this article at [www.ajnr.org](http://www.ajnr.org).

### REFERENCES

1. Fasano A, Espay AJ, Tang-Wai DF, et al. **Gaps, controversies, and proposed roadmap for research in normal pressure hydrocephalus.** *Mov Disord* 2020;35:1945–54 [CrossRef Medline](#)
2. Wang Z, Zhang Y, Hu F, et al. **Pathogenesis and pathophysiology of idiopathic normal pressure hydrocephalus.** *CNS Neurosci Ther* 2020;26:1230–40 [CrossRef Medline](#)
3. Bassi MA, Lopez MA, Confalone L, et al. **Normal pressure hydrocephalus: diagnosis and treatment.** *Nature* 2020;388:539–47 [CrossRef Medline](#)
4. Andersson J, Rosell M, Kockum K, et al. **Challenges in diagnosing normal pressure hydrocephalus: evaluation of the diagnostic guidelines.** *eNeurologicalSci* 2017;7:27–31 [CrossRef Medline](#)
5. Halperin JJ, Kurlan R, Schwab JM, et al. **Practice guideline: idiopathic normal pressure hydrocephalus: response to shunting and predictors of response.** *Neurology* 2015;85:2063–71 [CrossRef Medline](#)
6. Giordan E, Palandri G, Lanzino G, et al. **Outcomes and complications of different surgical treatments for idiopathic normal pressure hydrocephalus: a systematic review and meta-analysis.** *J Neurosurg* 2019;131:1024–36 [CrossRef Medline](#)
7. Bergsneider M, Black PML, Klinge P, et al. **INPH guidelines, part IV: surgical management of idiopathic normal-pressure hydrocephalus.** *Neurosurgery* 2005;57:S2–29–39 [CrossRef](#)
8. Bradley WG, Kortman KE, Burgoyne B. **Flowing cerebrospinal fluid in normal and hydrocephalic states: appearance on MR images.** *Radiology* 1986;159:611–16 [CrossRef Medline](#)
9. Pereira Damasceno B, Damasceno BP. **Normal pressure hydrocephalus: diagnostic and predictive evaluation.** *Dement Neuropsychol* 2015;9:350–55 [CrossRef Medline](#)
10. Ishikawa M, Oowaki H, Takezawa M, et al. **Disproportionately enlarged subarachnoid space hydrocephalus in idiopathic normal-pressure hydrocephalus and its implication in pathogenesis.** *Acta Neurochir Suppl* 2016;122:287–90 [CrossRef Medline](#)
11. Craven CL, Toma AK, Mostafa T, et al. **The predictive value of DESH for shunt responsiveness in idiopathic normal pressure hydrocephalus.** *J Clin Neurosci* 2016;34:294–98 [CrossRef Medline](#)
12. Grahne K, Jusue-Torres I, Szujewski C, et al. **The quest for predicting sustained shunt response in normal-pressure hydrocephalus: an analysis of the callosal angle's utility.** *World Neurosurg* 2018;115:e717–22 [CrossRef Medline](#)
13. Kockum K, Virhammar J, Riklund K, et al. **Diagnostic accuracy of the iNPH radscale in idiopathic normal pressure hydrocephalus.** *PLoS One* 2020;15:e0232275 [CrossRef Medline](#)
14. Kockum K, Lilja-Lund O, Larsson EM, et al. **The idiopathic normal-pressure hydrocephalus radscale: a radiological scale for structured evaluation.** *Eur J Neurol* 2018;25:569–76 [CrossRef Medline](#)
15. Relkin N, Marmarou A, Klinge P, et al. **Diagnosing idiopathic normal-pressure hydrocephalus.** *Neurosurgery* 2005;57(Suppl 3):S4–16 [CrossRef Medline](#)
16. Eklund A, Smielewski P, Chambers I, et al. **Assessment of cerebrospinal fluid outflow resistance.** *Med Biol Eng Comput* 2007;45:719–35 [CrossRef Medline](#)
17. Virhammar J, Laurell K, Cesarini KG, et al. **The callosal angle measured on MRI as a predictor of outcome in idiopathic normal-pressure hydrocephalus.** *J Neurosurg* 2014;120:178–84 [CrossRef Medline](#)
18. Virhammar J, Laurell K, Cesarini KG, et al. **Preoperative prognostic value of MRI findings in 108 patients with idiopathic normal pressure hydrocephalus.** *AJNR Am J Neuroradiol* 2014;35:2311–18 [CrossRef Medline](#)
19. Folstein MF, Folstein SE, McHugh PR. **“Mini-mental state”: a practical method for grading the cognitive state of patients for the clinician.** *J Psychiatr Res* 1975;12:189–98 [CrossRef Medline](#)
20. Hellström P, Klinge P, Tans J, et al. **A new scale for assessment of severity and outcome in iNPH.** *Acta Neurol Scand* 2012;126:229–37 [CrossRef Medline](#)
21. Landis JR, Koch GG. **The measurement of observer agreement for categorical data.** *Biometrics* 1977;33:159–74 [CrossRef Medline](#)

22. Kuchcinski G, Jacquiez C, Baroncini M, et al. Idiopathic normal-pressure hydrocephalus: diagnostic accuracy of automated sulcal morphometry in patients with ventriculomegaly. *Clin Neurosurg* 2019;85:E747–55 [CrossRef Medline](#)
23. Hong YJ, Kim MJ, Jeong E, et al. Preoperative biomarkers in patients with idiopathic normal pressure hydrocephalus showing a favorable shunt surgery outcome. *J Neurol Sci* 2018;387:21–26 [CrossRef Medline](#)
24. Kockum K, Virhammar J, Riklund K, et al. Standardized image evaluation in patients with idiopathic normal pressure hydrocephalus: consistency and reproducibility. *Neuroradiology* 2019;61:1397–406 [CrossRef Medline](#)
25. Laticevschi T, Lingenberg A, Armand S, et al. Can the radiological scale “iNPH radscale” predict tap test response in idiopathic normal pressure hydrocephalus? *J Neurol Sci* 2021;420:117239 [CrossRef Medline](#)
26. Agerskov S, Wallin M, Hellström P, et al. Absence of disproportionately enlarged subarachnoid space hydrocephalus, a sharp callosal angle, or other morphologic MRI markers should not be used to exclude patients with idiopathic normal pressure hydrocephalus from shunt surgery. *AJNR Am J Neuroradiol* 2019;40:74–79 [CrossRef Medline](#)
27. Kojoukhova M, Koivisto AM, Korhonen R, et al. Feasibility of radiological markers in idiopathic normal pressure hydrocephalus. *Acta Neurochir (Wien)* 2015;157:1709–19 [CrossRef Medline](#)
28. Shinoda N, Hirai O, Hori S, et al. Utility of MRI-based disproportionately enlarged subarachnoid space hydrocephalus scoring for predicting prognosis after surgery for idiopathic normal pressure hydrocephalus: Clinical research. *J Neurosurg* 2017;127:1436–42 [CrossRef Medline](#)
29. Yamada S, Ishikawa M, Nozaki K. Exploring mechanisms of ventricular enlargement in idiopathic normal pressure hydrocephalus: a role of cerebrospinal fluid dynamics and motile cilia. *Fluids Barriers CNS* 2021;18:20 [CrossRef Medline](#)
30. Modesto PC, Pinto FC. Home physical exercise program: analysis of the impact on the clinical evolution of patients with normal pressure hydrocephalus. *Arq Neuropsiquiatr* 2019;77:860–70 [CrossRef](#)
31. Shanks J, Markenroth Bloch K, Laurell K, et al. Aqueductal CSF stroke volume is increased in patients with idiopathic normal pressure hydrocephalus and decreases after shunt surgery. *AJNR Am J Neuroradiol* 2019;40:453–59 [CrossRef Medline](#)
32. Hamilton RB, Scalzo F, Baldwin K, et al. Opposing CSF hydrodynamic trends found in the cerebral aqueduct and prepontine cistern following shunt treatment in patients with normal pressure hydrocephalus. *Fluids Barriers CNS* 2019;16:2–13 [CrossRef Medline](#)
33. Ziegelitz D, Starck G, Kristiansen D, et al. Cerebral perfusion measured by dynamic susceptibility contrast MRI is reduced in patients with idiopathic normal pressure hydrocephalus. *J Magn Reson Imaging* 2014;39:1533–42 [CrossRef Medline](#)
34. Ziegelitz D, Arvidsson J, Hellström P, et al. Pre-and postoperative cerebral blood flow changes in patients with idiopathic normal pressure hydrocephalus measured by computed tomography (CT)-perfusion. *J Cereb Blood Flow Metab* 2016;36:1755–66 [CrossRef Medline](#)
35. Ziegelitz D, Arvidsson J, Hellström P, et al. In patients with idiopathic normal pressure hydrocephalus postoperative cerebral perfusion changes measured by dynamic susceptibility contrast magnetic resonance imaging correlate with clinical improvement. *J Comput Assist Tomogr* 2015;39:531–40 [CrossRef Medline](#)
36. Engel DC, Adib SD, Schuhmann MU, et al. Paradigm-shift: radiological changes in the asymptomatic iNPH-patient to be: An observational study. *Fluids Barriers CNS* 2018;15:5 [CrossRef Medline](#)
37. Kimihira L, Iseki C, Takahashi Y, et al. A multi-center, prospective study on the progression rate of asymptomatic ventriculomegaly with features of idiopathic normal pressure hydrocephalus on magnetic resonance imaging to idiopathic normal pressure hydrocephalus. *J Neurol Sci* 2020;419:117166 [CrossRef Medline](#)
38. Suehiro T, Kazui H, Kanemoto H, et al. Changes in brain morphology in patients in the prediagnostic stage of idiopathic normal pressure hydrocephalus. *Psychogeriatrics* 2019;19:557–65 [CrossRef Medline](#)
39. Czepko R, Cieslicki K. Repeated assessment of suspected normal pressure hydrocephalus in non-shunted cases: a prospective study based on the constant rate lumbar infusion test. *Acta Neurochir (Wien)* 2016;158:855–63 [CrossRef Medline](#)
40. Wu D, Moghekar A, Shi W, et al. Systematic volumetric analysis predicts response to CSF drainage and outcome to shunt surgery in idiopathic normal pressure hydrocephalus. *Imaging Informatics and Artificial Intelligence*. <https://doi.org/10.1007/s00330-020-07531-z>. Accessed March 18, 2021
41. Rau A, Kim S, Yang S, et al. SVM-based normal pressure hydrocephalus detection. *Clin Neuroradiol* 2021 Jan 26. [Epub ahead of print] [CrossRef](#)
42. Irie R, Otsuka Y, Hagiwara A, et al. A novel deep learning approach with a 3D convolutional ladder network for differential diagnosis of idiopathic normal pressure hydrocephalus and Alzheimer's Disease. *Magn Reson Med Sci* 2020;19:351–58 [CrossRef Medline](#)